An application of infrared analysis to determine the mineralogical phases formation in fluxes for thin slab casting of steel

Alejandro Cruz-Ramírez *, Julio Romo-Castañeda, María de los Ángeles Hernández-Pérez, Marissa Vargas-Ramírez, Antonio Romero-Serrano, Manuel Hallen-López

Metallurgy and Materials Department, Instituto Politécnico Nacional-ESIQIE, Apdo. P. 118-431, 07051 México D.F., Mexico

ARTICLE INFO

ABSTRACT

The Fourier Transformed Infrared (FTIR) spectra analysis of two fluxes used in the thin slab casting process of steel were carried out in order to identify the mineralogical species present in fluxes as received and after a heat treatment to 1573 K and further solidification at two different cooling velocities. Fluxes as received show the presence of wollastonite ($CaO \cdot SiO_2$) and a sodium carbonate (Na_2CO_3) as the main components; after the heat treatment, there was almost a whole transformation from the original compounds to cuspidine ($3CaO \cdot 2SiO_2 \cdot CaF_2$) and nepheline ($Na_2O \cdot Al_2O_3 \cdot 2SiO_2$) phases. These results were confirmed by X-ray powder diffraction (XRD) to the slowly cooling velocity. The FTIR technique is proposed as a useful and complementary technique to X-ray diffraction to study the structure of commercial fluxes for thin slab casting.

1. Introduction

Mold powders for thin slab casting process are composed mainly of oxides, alkaline and alkaline-earth metals with important contents of fluorides and carbon generally based on the SiO_2–CaO–CaF_2–Na_2O system. They are used in continuous casting of steel slabs, where they play an important role in the surface quality of the steel product and in the overall efficiency of the continuous casting process control [1]. It is well known that molten fluxes are based on the silicate melt which consists of three dimensional tetrahedrally bonded Si–O networks. The chemical composition and the physical form of the flux can control the melting temperature, melting rate, viscosity and surface tension of the flux. It has been found that viscosity and the melting temperature of the mold flux are increased when silica and alumina are added to the original composition of mold fluxes [2–4]. Alumina is an amphoter oxide but in mold slags with a large amount of alkali and alkaline earth oxides it will become a network former. Although the addition of alumina to pure silicate melts decreases viscosity, in most mold flux compositions alumina is anionic and increases the chain length and consequently the viscosity of the slag system [3]. The size of the silicate or aluminosilicate network in casting powders or slags become larger with increasing SiO_2 and Al_2O_3 contents, hence their mobility decreases resulting in a higher viscosity. The addition of alkali-metal oxides, such as Na_2O to the

mold flux, leads to the breakdown of the silicate network, resulting in lower viscosity. However, when the Na_2O contents are lower than Al_2O_3, there is a combination of Na^+ with Al^{3+} occupying the center of $(AlO_4)^{5-}$ tetrahedra instead of breaking silica network [5]. There are considerable variations in the constituents used by powder manufacturers, and when the casting powders are heated the constituents react to form different mineralogical phases [6]. The structure of MO–SiO_2 (MO represents a basic oxide) systems has been extensively studied by metallurgist, glass scientists, and mineralogist; however, the CaF_2 addition to this system presents some contradictory results. Contrary to Na_2O, the addition of fluoride as CaF_2 to mold fluxes considerably reduced the viscosity, the melting point and the activation energy. However, the opposite behavior was observed when CaF_2 is present in higher quantities in mold fluxes, this is due to the fluoride capability of surpassing crystallization [5,6]. Tsunawaki et al. [7] concluded that the addition of CaF_2 to the CaO–SiO_2 system in contents less than 20 mol% with a CaO/SiO_2 ratio less than unity, contributed to the breakage of some Si–O bonds as was observed in a Raman spectra study. Luth [8] suggested that the substitution of fluorine for oxygen ions in the SiO_2–CaO–CaF_2 system increased the degree of polymerization due to the formation of Ca–F complexes. Ueda et al. [9] determined that fluorine ions would not affect the wavenumber of silicate Infrared bands. The effect of CaF_2 on the modification of silicate network in the silicate melts is not clear yet, especially in basic slags in steelmaking processes. Cuspidine ($3CaO \cdot 2SiO_2 \cdot CaF_2$) is one of the most important crystallized compounds in mold flux film during thin slab casting process. Watanabe et al. [10] determined the primary crystallization field and the melting

---

temperature of cuspidine. Differential thermal analysis have been carried out in order to determine the changes in thermal properties of mold flux [11,12]. Recently, Dapiaggi et al. [13] developed a kinetic analysis on the cuspidine crystallization with differential thermal analysis of mold flux slag. In this work, the Fourier transform infrared spectroscopy (FTIR) is proposed as a useful and complementary technique, to X-ray diffraction, to study the structure of commercial fluxes for thin slab casting.

2. Experimental

Two commercial mold fluxes (named A1 and A2) used in an integrated steelmaking shop were studied. The samples were analyzed as received and after a heat treatment at 1573 K with different cooling rates. Table 1 shows the chemical composition of both powders which are used to produce medium carbon (0.07–0.1%C) and peritectic (0.09–0.15%C) steel.

2.1. Specimen preparation

In order to know the degree of crystallinity, 30 g of each flux were contained in a platinum crucible and heated up to 1573 K in a Lindberg/Blue STF54434C tube furnace with $MoSi_2$ heating elements and then cooled at two different rates. In one experiment, the fluxes were cooled slowly ($\sim$3 K/min) inside the furnace and in the other test they were rapidly cooled ($\sim$250 K/min) by pouring the molten flux on a copper plate. Finally, the slag obtained was crushed to the size less than 100 μm and analyzed by X-ray powder diffraction and FTIR spectroscopy.

2.2. X-ray-diffraction

The samples were analyzed in an X-ray Bruker D8 Focus with monochromatic Cu Kα radiation working in $\theta/2\theta$ configuration. Data were collected in an angular range from 20 to 100° with a step size of 0.02° and a counting time of 2 min^{-1}.

2.3. Fourier Transformed Infrared spectra measurements

The structure of the fluxes was analyzed by FTIR spectroscopy. Absorbance spectra were recorded with a Perkin Elmer System 2000 in the 4000–400 cm^{-1} range with a resolution of 2 cm^{-1}. 2 mg of each flux was mixed with 200 mg of KBr in an agate mortar, and then pressed with a load of 120 kg/cm^2 into pellets of 12 mm diameter. The spectrum of each sample represents an average of 32 scans. FTIR absorbance spectra analysis was carried out to evaluate the cuspidine phase formation. Synthetic cuspidine was prepared by melting 200 g of a mixture of SiO_2, $CaCO_3$ and CaF_2 in stoichiometric proportions in a platinum crucible at 1450 K, as it was reported by Hill et al. [12]. The reaction system was protected

by purified argon gas during the heating process with a flow rate of 150 cm^3/min. The molten flux was poured on a copper plate. The cuspidine formation was confirmed by X-ray diffraction analysis (XRD). Losses in fluorine content have not been accounted for.

3. Results and discussion

The XRD patterns of the tested fluxes are shown in Figs. 1 and 2 for fluxes A1 and A2, respectively. The powders as received show simple chemical compounds such as $CaCO_3$, C, CaF_2, Na_2CO_3. It is also observed the presence of wollastonite ($CaO \cdot SiO_2$), which appears in both fluxes as received. It is known that these chemical compounds are present in minerals like feldspars, clays, limestone, fluorspar and graphite [14]. When both fluxes were heated to 1573 K and cooled slowly, two mineralogical phases were formed: these are the cuspidine ($3CaO \cdot 2SiO_2 \cdot CaF_2$) and nepheline ($Na_2O \cdot Al_2O_3 \cdot 2SiO_2$) with small amounts of limestone ($CaCO_3$) and fluorite (CaF_2). The quantity of these phases was different in each flux, according to their original chemical composition. The cooling velocity affects the formation of phases; for the slow cooling velocity, there were almost whole transformations from the original compounds to cuspidine and nepheline phases, whereas the fast cooling velocity did not produce crystalline phases. The IR spectra of the fluxes as received are shown in Fig. 3. Two main minerals were detected in both fluxes; these are wollastonite ($CaO \cdot SiO_2$) and sodium carbonate (Na_2CO_3). The bands observed at 1440 and 881 cm^{-1} correspond to sodium carbonate [15–17]. The bands located at about 1057, 1012, 961, 910, 680, 650 and 451 cm^{-1} are assigned to the vibrations of the

Table 1
Chemical composition of commercial mold powders.

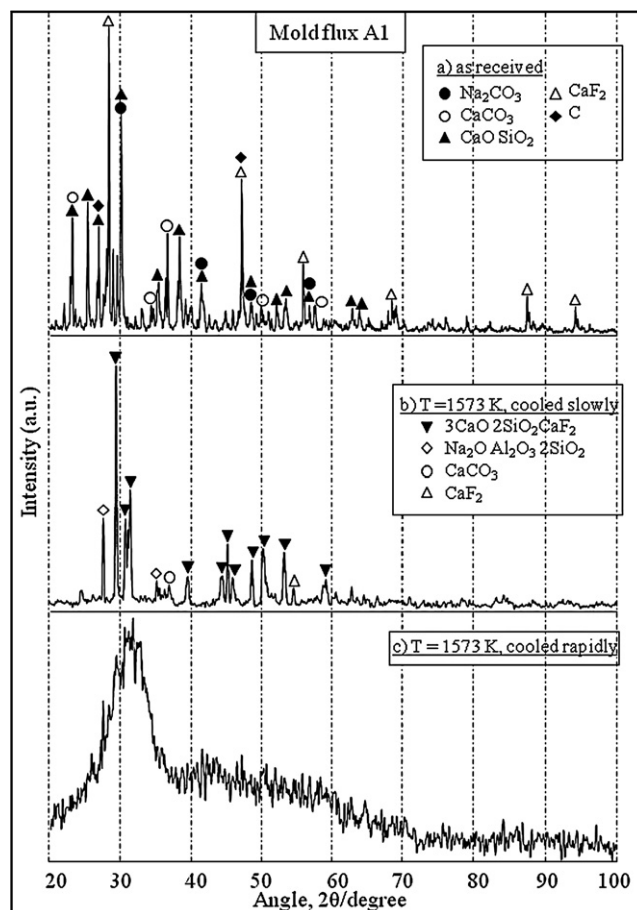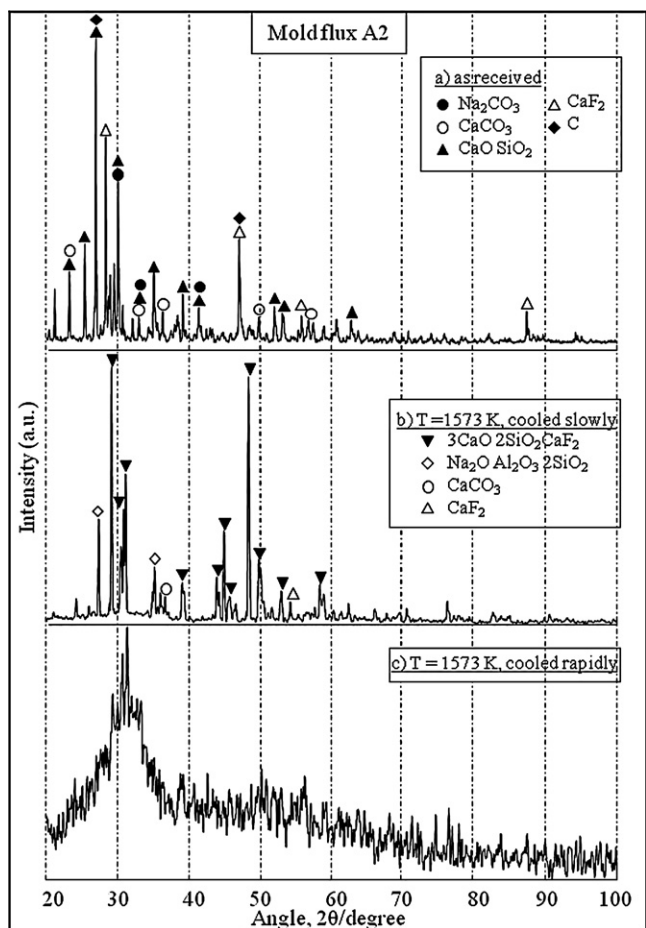| Chemical compounds	Mold fluxes (wt%)	
	A1	A2
SiO_2	27.04	25.51
CaO	28.85	29.71
MgO	2.06	1.97
Al_2O_3	2.08	2.09
Fe_2O_3	0.59	0.41
MnO	0.04	2.92
Na_2O	11.7	9.36
K_2O	0.73	0.38
CaF_2	21.84	22.1
C_{total}	4.97	5.04
H_2O	0.40	0.50

Fig. 1. X-ray powder diffraction of the A1 flux, (a) as received, (b) heat treated to 1573 K and cooled slowly and (c) heat treated to 1573 K and cooled rapidly.

Fig. 2. X-ray powder diffraction of the A2 flux, (a) as received, (b) heat treated to 1573 K and cooled slowly and (c) heat treated to 1573 K and cooled rapidly.

Fig. 3. FTIR spectra of the commercial fluxes as received.

wollastonite phase [16–18]. The fluorite contribution to the composition of the commercial fluxes is high, 22 wt%, even though its principal absorption is located at 280 cm^{-1}, so it is not observed in the wavenumber range studied [15,19]. Concerning to the minor components of the fluxes, such as K_2O, MgO, MnO, Al_2O_3 and Fe_2O_3, they were in a very low quantity to be observed in the IR spectra. In addition, almost all these oxides have a broad strong absorbance peak in the 500–300 cm^{-1} range, which makes difficult to distinguish the contribution of each oxide. The FTIR of both fluxes are quite similar, but the high intensity of the bands located in the 550–420 cm^{-1} range in the spectrum of the A2 flux can be attributed to the content of MnO (see Table 1) which is absent in the A1 flux. The synthetic cuspidine obtained was glassy and slightly cloud. The X-ray powder diffraction showed that it is a crystalline phase and approximately 100% cuspidine. Synthetic cuspidine and both commercial fluxes have saturation compositions. The mol% of the cuspidine components in the A1 and A2 fluxes were calculated from the chemical composition analysis taking into account only the CaO, SiO_2 and CaF_2 quantities. The obtained mol ratios CaO/SiO_2/CaF_2 were 41.4/36.2/22.4 and 42.9/34.4/22.7 for A1 and A2 fluxes, respectively. The mol% for synthetic cuspidine with $3CaO \cdot 2SiO_2 \cdot 1CaF_2$ molecules was 50/33.3/16.7. In general, the absorption bands of cuspidine can be grouped in several kinds of bands corresponding to the stretching vibrations of the [Si–O_4]-tetrahedra [9,20–23]. These groups are observed in the 1220–760 cm^{-1} range and correspond to the vibration of [Si–O_4]-tetrahedra with 1, 2, 3 and 4 non-bridging oxygen per silicon (NBO/Si). For synthetic cuspidine these groups of bands are located at 1100–1031 cm^{-1} (1100, 1063 and 1030 cm^{-1}) for [Si–O_4]-tetra-
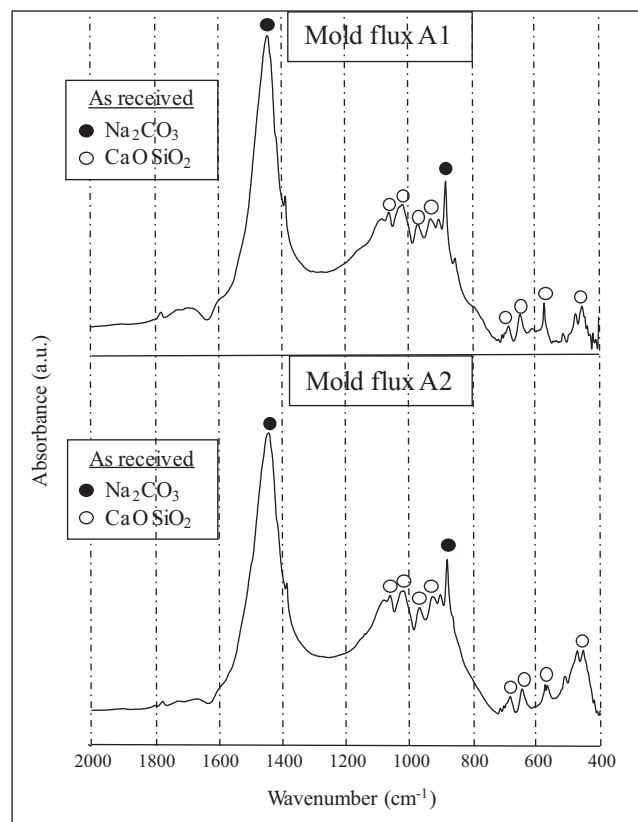
hedra with 1 NBO/Si, at 985 cm^{-1} (2 NBO/Si), 948–916 cm^{-1} (3 NBO/Si) and 856 cm^{-1} (4 NBO/Si). The bands observed at 716, 653, 555–510 and 430 cm^{-1} can be attributed to $[Si_2O_7]^{6-}$-dimer, $[SiF_6]^{2-}$-octahedral complexes, Si–O bonding and Ca–O, respectively [22]. In particular, the group of bands assigned to [Si–O_4]-tetrahedra with 1 NBO/Si could contain some contribution from the Si–F bond which absorbs at 945 cm^{-1} (Fig. 4).

The A1 and A2 fluxes, show comparable results but only the results of flux A2 are shown in Fig. 5. The spectra of the fluxes slowly cooled and rapidly cooled are very similar; they show the absorption bands of cuspidine and nepheline phases, as seen in
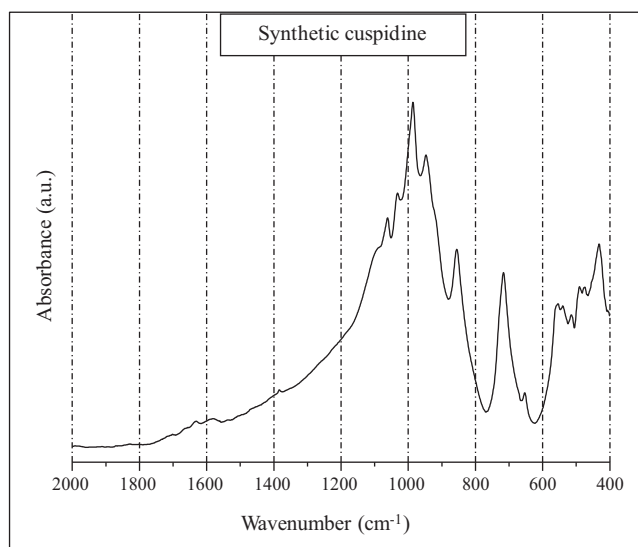

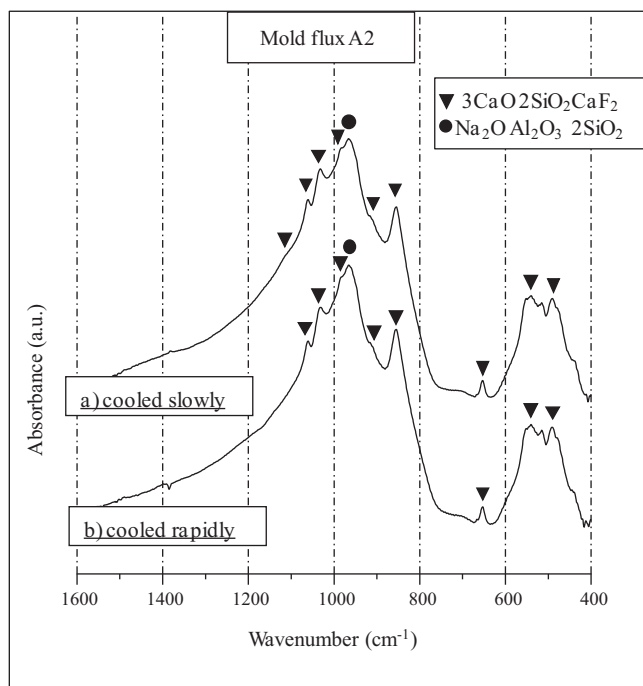**Fig. 4.** FTIR spectrum of the synthetic cuspidine.

Fig. 5. FTIR spectra of the A2 flux, (a) heat treated to 1573 K and cooled slowly and (b) heat treated to 1573 K and cooled rapidly. ▼ Cuspidine and ● Nepheline absorption bands.

DRX spectra. However, there is not signal from $CaCO_3$ or CaF_2 in FTIR spectra. A small difference is observed in the commercial fluxes, the shoulder observed in synthetic cuspidine corresponds to one of the absorptions of $[Si–O_4]$-tetrahedra with 1 NBO/Si and it is shifted to higher wavenumbers ($1119\ cm^{-1}$) in the flux slowly cooled and it is absent in the flux rapidly cooled. This could be attributed to the crystallinity of the flux slowly cooled and to the amorphous condition of the flux rapidly cooled. The cooled fluxes present the stretching vibrations of $[Si–O_4]$-tetrahedra at 1120–1030, 985, 948 (shoulder) and $856\ cm^{-1}$ for 1, 2, 3 and 4 NBO/Si, respectively. A high intensity peak corresponding to nepheline phase is observed at $965\ cm^{-1}$ [19]. Nepheline formation has been observed in fluxes with alumina and Na_2O [6]. The intensity of the band assigned to the $[Si_2O_7]^6$-dimer in the cuspidine spectrum is very low in the spectrum of the A2 flux. This can be due to the influence of nepheline and the minor components presents in the commercial fluxes which interfere in the formation of the dimer. The Si–O bending vibration is observed at $600–450\ cm^{-1}$ and Ca–O bending absorption is not present in A2 flux.

The FTIR technique provides complementary information to DRX in the mineralogical phase detection. In this work, cuspidine and nepheline formation was detected by FTIR and DRX in commercial fluxes cooled at different rates but the presence of CaF_2 and $CaCO_3$ was not detected by FTIR. Mold fluxes present a great amount of characteristics lines in the XRD pattern, usually with a high noise level that difficult the spectrum analysis. For the FTIR technique, the signal to noise ratio is better than XRD. However,

the data source for inorganic compounds like minerals and mineralogical phases is very limited for the FTIR technique. A systematic analysis of the content of nepheline in melted and cooled fluxes should be carried out in order to establish its presence and interactions in the cuspidine–nepheline mixture.

4. Conclusions

The FTIR spectroscopy is a useful and complementary technique to X-ray diffraction to study the structure of commercial fluxes for thin slab casting. FTIR and XRD analysis confirm that the principal components of commercial fluxes are sodium carbonate and wollastonite and that the heat treatment at 1573 K induces the formation of cuspidine and nepheline phases. The nepheline and minor components in commercial fluxes affect the formation of $[Si_2O_7]^6$-dimer. The crystallinity of the flux slowly cooled can induce the shift to higher wavenumbers of the $[Si–O_4]$-tetrahedra with 1 NBO/Si absorption bands.

References

[1] J. Kromhout, A. Kamperman, M. Kick, J. Trouw, VII International Conference on Molten, Slags, Fluxes and Salts, 2004, 731–736.
[2] P. Grieveson, S. Bagha, N. Machingawuta, K. Liddell, K.C. Mills, Ironmaking and Steelmaking 15 (4) (1988) 181–186.
[3] R. Bommaraju, Steelmaking Conference Proc., ISS-AIME, vol. 74, 1991, 131–146.
[4] J.H. Park, D.J. Min, Journal of Non-Crystalline Solids 337 (2004) 150–156.
[5] H. Chang, T. Lee, E. Tatsuhiko, Transactions ISIJ 27 (1987) 797–804.
[6] A. Cruz, F. Chávez, A. Romero, E. Palacios, V. Arredondo, Journal of Materials Processing Technology 182 (1–3) (2007) 358–362.
[7] Y. Tsunawaki, N. Iwamoto, T. Hattori, A. Mitsuishi, Journal of Non-Crystalline Solids 44 (1981) 369–378.
[8] R.W. Luth, American Mineralogist 73 (1988) 297–305.
[9] S. Ueda, H. Koyo, T. Ikeda, Y. Kariya, M. Maeda, ISIJ International 40 (2000) 739.
[10] T. Watanabe, H. Fukuyama, K. Nagata, ISIJ International 42 (5) (2002) 489–497.
[11] R. Soares, M. Fonseca, R. Neuman, V. Meneses, A. Lavinas, J. Dweck, Termochimica Acta 318 (1998) 131–136.
[12] R.G. Hill, N. Da Costa, R.V. Law, Journal of Non-Crystalline Solids 351 (2005) 69–74.
[13] M. Dapiaggi, G. Artioli, C. Righi, R. Carli, Journal of Non-Crystalline Solids 353 (2007) 2852–2860.
[14] A. Cruz, F. Chávez, A. Romero, E. Palacios, Mineral Processing and Extractive Metallurgy (Trans. Inst. Metall. C) 116 (1) (2007) 65–71.
[15] R.A. Nyquist, R.O. Kagel, Infrared Spectra of Organic Compounds, Academic Press, USA, 1971.
[16] FDMSpectra database. http://www.fdmspectra.com.
[17] NIST Chemistry webbook data base. http://weebbook.nist.gob/chemistry/.
[18] R.P. Sreekanth Chakradhar, B.M. Nagabhushana, G.T. Chandrappa, K.P. Ramesh, J.L. Rao, Materials Chemistry and Physics 95 (2006) 169–175.
[19] M.V. Zeller, M.P. Juszli, Reference Spectra of Minerals, Perkin Elmer Infrared Bulletin, USA, 1975.
[20] S.A. MacDonald, C.R. Schardt, D.J. Masiello, J.H. Simmons, Journal of Non-Crystalline Solids 275 (2000) 72–82.
[21] F. Branda, F. Arcobello-Varlese, A. Constantini, G. Luciani, Journal of Non-Crystalline Solids 246 (1999) 27–33.
[22] J.H. Park, D.J. Min, H.S. Song, ISIJ International 42 (4) (2002) 344–351.
[23] J.H. Park, D.S. Kim, Y.D. Lee, H.S. Song, D.J. Min, VII International Conference on Molten Slags and Salts, The South African Institute of Mining and Metallurgy, (2004), pp. 157–164.